***For correspondence***
*Name*: Kensuke Nishioka
*Address*: Japan Advanced Institute of Science and Technology,
Asahidai 1-1, Tatsunokuchi, Ishikawa, 923-1292, JAPAN
*Tel/Fax/E-mail*: +81-761-51-1562 / +81-761-51-1149 / nishioka@jaist.ac.jp

# Annual Output Estimation of Concentrator Photovoltaic Systems Using High-Efficiency InGaP/InGaAs/Ge Triple-Junction Solar Cells Based on Experimental Solar Cell's Characteristics and Field-Test Meteorological Data

Kensuke Nishioka[1], Tatsuya Takamoto[2], Takaaki Agui[2], Minoru Kaneiwa[2],
Yukiharu Uraoka[1] and Takashi Fuyuki[1]
[1]Graduate School of Materials Science, Nara Institute of Science and Technology
8916-5 Takayama, Ikoma, Nara 630-0101, Japan
[2]SHARP Corporation
282-1 Hajikami, Shinjo-cho, Kitakatsuragi-gun, Nara 639-2198, Japan

## ABSTRACT

The temperature dependences of the electrical characteristics of InGaP/InGaAs/Ge triple-junction solar cells under concentration were evaluated. For these solar cells, conversion efficiency ( $\eta$ ) decreased with increasing temperature, and increased with increasing concentration ratio owing to an increase in open-circuit voltage. The decrease in $\eta$ with increasing temperature decreases with increasing concentration ratio. Moreover, the annual output of a concentrator system with a high-efficiency triple-junction cell is estimated utilizing the experimental solar cell's characteristics obtained in this study and field-test meteorological data collected for one year at the Nara Institute of Science and Technology, and compared with that of a nonconcentration flat-plate system.

**KEYWORDS**: multijunction solar cell, temperature coefficient, concentration, annual output

## 1. INTRODUCTION

Multijunction solar cells consisting of InGaP, (In)GaAs and Ge are known as super-high efficiency and are now used for space applications. Multijunction cells lattice-matched to Ge substrates have been improved and their conversion efficiency has reached 31% (AM1.5G) owing to their lattice-matched configuration [1, 2]. Therefore, concentrator photovoltaic systems using high-efficiency solar cells are one of the important issues in the development of an advanced PV system. The production cost of multijunction solar cells composed of III-V materials is higher than that of Si solar cells. However, the necessary cell size decreases with increasing concentration ratio, thus reducing the total cost of concentrator systems will decrease. High-efficiency multijunction cells under high concentrations have been investigated for terrestrial applications [3, 4]. Also, for low-concentration operation, multijunction cells have been investigated for space satellite use [5-7].

It is considered that the temperature of solar cells increases under light-concentrating operations. Such cells, if insulated, are potentially heated to 1400$^{o}$C at 500 suns concentration [8]. Their conversion efficiency decreases when their temperature increases [9, 10]. Though passive cooling methods with a heat sink [11] or a heat spreader [12] have been favored for cost and reliability purposes, they could not completely suppress this increase in temperature.

However, the temperature characteristics of InGaP/InGaAs/Ge triple-junction solar cells under concentration have not been evaluated in detail. In this study, we have evaluated such temperature characteristics under concentration conditions.

The annual output of a concentrator system with a high-efficiency triple-junction cell is estimated utilizing field-test meteorological data collected for one year at the Nara Institute of Science and Technology (NAIST, Japan) and experimental cell characteristics

obtained in this study, and compared with that of a nonconcentration flat-plate system. Then, the possibilities of concentrator systems are discussed.

## 2. InGaP/InGaAs/Ge TRIPLE-JUNCTION SOLAR CELL

Figure 1 shows a schematic illustration of the InGaP/InGaAs/Ge triple-junction cell evaluated in this study. The subcells (InGaP junction, InGaAs junction and Ge junction of this cell) were grown on a *p*-type Ge substrate using metal-organic chemical vapor deposition. The $In_{0.49}Ga_{0.51}P$ top subcell, $In_{0.01}Ga_{0.99}As$ middle subcell, and Ge bottom subcell were all lattice-matched. The InGaP subcell was connected to the InGaAs cell by a *p*-AlGaAs/*n*-InGaP tunnel junction. The InGaAs subcell was connected to the Ge cell by a *p*-GaAs/*n*-GaAs tunnel junction. The electrodes were fabricated by evaporation. The electrode consisted of a 5-μm-thick Ag. The width and pitch of the grid electrodes were 7 μm and 120 μm (optimized for high-concentration operations), respectively.

## 3. TEMPERATURE CHARACTERISTICS OF TRIPLE-JUNCTION SOLAR CELL UNDER CONCENTRATED LIGHT

Light from the solar simulator (Light source: Xe lamp) was adjusted to 1 sun (AM 1.5G, 100 mW/cm$^2$), and focused by a Fresnel lens. Concentration ratio was determined by dividing short-circuit current ($I_{sc}$) under concentrated light by $I_{sc}$ under 1 sun illumination. It was varied from 1 sun to 200 suns. The cell was attached to a thermostat stage by a solder with high heat conductivity. The temperature dependences of the solar cell's characteristics were investigated in the temperature range from 30°C to 120°C.

Table 1 shows the characteristics of the solar cell at 25°C for various concentration ratios (1 sun, 17 suns and 200 suns). Figures 2(a)-(d) show the temperature dependences of the characteristics ((a) open-circuit voltage: $V_{oc}$, (b) short-circuit current: $I_{sc}$, (c) fill factor:

*FF* and (d) conversion efficiency: $\eta$) of the InGaP/InGaAs/Ge triple-junction solar cell. Table 2 shows the temperature coefficients of these characteristics ($dX/dT$: $X$ means $V_{oc}$, $I_{sc}$, *FF* and $\eta$) and the temperature coefficients normalized by the same parameter at 25°C ($(dX/dT)/X_{(25°C)} \times 100$).

Figure 2(a) shows the temperature dependence of $V_{oc}$. For all concentration ratios, $V_{oc}$ decreased with increasing temperature.

The *I*-*V* characteristics of the solar cell are expressed by

$$I = I_0 \left\{ \exp\left( \frac{qV}{nkT} \right) - 1 \right\} - I_{sc}, \qquad (1)$$

where $I_0$, $q$, $n$, $k$ and $T$ are the saturation current, elementary charge, diode ideality factor, Boltzmann constant and absolute temperature, respectively.

From eq. (1), $V_{oc}$ ($I$=0) is given by

$$V_{oc} = \frac{nkT}{q} \ln\left( \frac{I_{sc}}{I_0} + 1 \right). \qquad (2)$$

From eq. (2), it is considered that the temperature characteristic of saturation current ($I_0$) markedly influences the temperature characteristic of $V_{oc}$. The saturation current density ($J_0$) is given by

$$J_0 = q\left( \frac{D_e}{\tau_e} \right)^{1/2} \frac{n_i^2}{N_A} \left\{ \frac{S_e(\tau_e / D_e)^{1/2} \cosh(x_p / \sqrt{D_e \tau_e}) + \sinh(x_p / \sqrt{D_e \tau_e})}{S_e(\tau_e / D_e)^{1/2} \sinh(x_p / \sqrt{D_e \tau_e}) + \cosh(x_p / \sqrt{D_e \tau_e})} \right\}$$

$$+ q\left( \frac{D_h}{\tau_h} \right)^{1/2} \frac{n_i^2}{N_D} \left\{ \frac{S_h(\tau_h / D_h)^{1/2} \cosh(x_n / \sqrt{D_h \tau_h}) + \sinh(x_n / \sqrt{D_h \tau_h})}{S_h(\tau_h / D_h)^{1/2} \sinh(x_n / \sqrt{D_h \tau_h}) + \cosh(x_n / \sqrt{D_h \tau_h})} \right\}, \qquad (3)$$

where $n_i$ is the intrinsic carrier concentration, $N_A$ and $N_D$ are the acceptor and donor concentrations, $S_h$ and $S_e$ are the surface-recombination velocities in the *n*- and *p*-type materials, $x_p$ and $x_n$ are the thicknesses of the *p*- and *n*-type layers, $D_e$ and $D_h$ are the diffusion constants of electrons and holes, and $\tau_e$ and $\tau_h$ are the lifetimes of electrons and

holes, respectively. $J_0$ strongly depends on $T$ through its proportionality to the square of $n_i$. $n_i$ is expressed by

$$n_i^2 = 4M_c M_v (2\pi kT/h^2)^3 (m_e^* m_h^*)^{3/2} \exp(-E_g/kT), \quad (4)$$

where $M_c$ and $M_v$ are the numbers of equivalent minima in the conduction and valence bands, $h$ is Planck's constant, and $m_e^*$ and $m_h^*$ are the effective masses of electrons and holes, respectively.

From eqs. (2)-(4), it is found that the decrease in $V_{oc}$ with increasing temperature arises mainly from the change in $n_i$. $J_0$ increases exponentially with decreasing $1/T$, and $V_{oc}$ decreases almost linearly with increasing $T$. $D_e$, $D_h$, $\tau_e$ and $\tau_h$ are all temperature-dependent, and the temperature dependence of $J_0$ is slightly influenced by their temperature dependences.

Moreover, $V_{oc}$ increases with increasing concentration ratio. From eq. (2), $V_{oc}$ increases logarithmically with radiation intensity [13-16]. It is found that the decrease in $V_{oc}$ with increasing temperature ($dV_{oc}/dT$) gets smaller with increasing concentration ratio, as shown in Table 2.

For the $n^+/p$ junction, $J_0$ is approximated as

$$J_0 \cong q\left(\frac{D_e}{\tau_e}\right)^{1/2} \frac{n_i^2}{N_A}. \quad (5)$$

$D_e$ and $\tau_e$ in eq. (5) are all temperature-dependent. If $D_e / \tau_e$ is proportional to $T^\gamma$, where $\gamma$ is a constant, then from eqs. (4) and (5)

$$J_0 \propto T^{(3+\gamma/2)} \exp\left(-\frac{E_g(T)}{kT}\right), \quad (6)$$

where $E_g(T)$ is the band-gap energy at $T$ and the temperature dependence exponent $(3+\gamma/2)$ is from the third-order dependence of $n_i^2$ and $\gamma$-order dependence of $D_e / \tau_e$.

The variation in bandgap with absolute temperature is expressed as [17]

$$E_g(T) = E_g(0) - \frac{\alpha T^2}{T+\beta} \quad , \tag{7}$$

where $\alpha$ and $\beta$ are constants.

The differentiation of eq. (2) with respect to $T$ and the substitution of band-gap voltage ($V_g(T)$) for $E_g(T)/q$ result in

$$\frac{dV_{oc}}{dT} = -\left(\frac{V_g(T) - V_{oc} + (3+\gamma/2)V_T}{T}\right) + V_T\left(\frac{1}{I_{sc}}\frac{dI_{sc}}{dT} + \frac{1}{V_T}\frac{dV_g(T)}{dT}\right) \quad , \tag{8}$$

where $V_T$, the thermal voltage, is substituted for $kT/q$. The second term in eq. (8) can be neglected compared with the first term. Therefore, the temperature dependence of $V_{oc}$ is approximated as [10]

$$\frac{dV_{oc}}{dT} = -\left(\frac{V_g(T) - V_{oc} + (3+\gamma/2)V_T}{T}\right) \quad . \tag{9}$$

The dominant part of this equation is ($V_g(T)$- $V_{oc}$), and we can see that the temperature dependence of $V_{oc}$ is smaller for solar cells with a large $V_{oc}$. Therefore, the decrease in $V_{oc}$ with increasing temperature decreased because of the increase in $V_{oc}$ with increasing concentration ratio.

Figure 2(b) shows the temperature dependence of $I_{sc}$. The increase in minority-carrier diffusion length and the shift in optical absorption edge energy with increasing temperature produce a small increase in $I_{sc}$. An increase in $I_{sc}$ with increasing temperature results from the change in absorption coefficient with temperature.

Figure 2(c) shows the temperature dependence of *FF*. *FF* decreased with increasing temperature, and increased with increasing concentration ratio. *FF* at 200 suns is smaller than that at 17 suns because of the influence of series resistance. The temperature dependence of *FF* is mainly derived from the temperature dependence of $V_{oc}$.

Figure 2(d) shows the temperature dependence of $\eta$. The temperature dependence of $\eta$ is mostly affected by the temperature dependence of $V_{oc}$. For all concentration ratios, $\eta$ decreased with increasing temperature, and increased with increasing concentration ratio because of the increase in $V_{oc}$. The normalized temperature coefficient of the conversion efficiency of the InGaP/InGaAs/Ge triple-junction solar cell $((d\eta/dT)/\eta_{(25°C)} \times 100)$ is -0.248%/$^{o}$C at 1 sun, as shown in Table 2. On the other hand, the normalized temperature coefficient of the conversion efficiency of a crystalline-silicon solar cell is -0.4 or -0.5%/$^{o}$C under 1 sun operation. This indicates that InGaP/InGaAs/Ge triple-junction solar cells have an advantage over crystalline-silicon solar cells under high-temperature conditions. Moreover, the decrease in $\eta$ with increasing temperature decreases with increasing concentration ratio. These results indicate that concentration operations have beneficial effects on high-temperature operations.

## 4. ESTIMATION OF ANNUAL OUTPUT

A nonconcentration flat-plate 50-kW PV system was installed at NAIST. This system automatically measured meteorological data and operating condition data in 200 channels at an interval of 6 sec, and the data were stored in a database. A pyrheliometer, a pyranometer, a spectroradiometer, a rain gauge, a wind speed meter, and a thermometer were used to measure meteorological data. In this study, the annual data from August 1999 to July 2000 were adopted.

Figure 3 shows the diffuse irradiation and direct irradiation for each month. The direct irradiation was approximately half of the global irradiation (the sum of diffuse irradiation and direct irradiation). Nonconcentration flat-plate systems can utilize both diffuse and direct irradiations, while concentrator systems can utilize only direct irradiation. Thus, it is important to compare the annual output of concentrator systems composed of superhighly

efficient InGaP/InGaAs/Ge triple-junction solar cells with that of the nonconcentration systems composed of Si solar cells.

In this study, the annual output energies of a 17 sun concentrator system and a 200 sun concentrator system per 1 $m^2$ irradiation area were estimated based on the experimental cell characteristics (described in the previous section) and field-test meteorological data (observed at NAIST). For comparison with that of a flat-plate system, the annual output energy of a nonconcentration flat-plate system composed of single-crystalline Si solar cells per 1 $m^2$ irradiation area was estimated.

The output energy of a flat-plate PV system is expressed by [18]

$$P_{out} = K_T \cdot K_f \cdot P_g \cdot \eta_s , \qquad (10)$$

where $P_{out}$ is the output energy, $P_g$ is the global irradiation (diffuse irradiation + direct irradiation), $\eta_s$ is the $\eta$ under the standard test conditions (100-mW/$cm^2$ irradiation, 25°C module temperature, and AM1.5 global spectrum), and $K_f$ is the correction coefficient for all factors except temperature. In this brief estimation, $K_f$ was assumed to be 1. When the standard temperature is set to 25°C, the correction coefficient for temperature $K_T$ is

$$K_T = 1 + a\,(T_m - 25), \qquad (11)$$

where $T_m$ [°C] is the module temperature and $a$ is the normalized temperature coefficient ($(d\eta/dT)/\eta_{(25°C)} \times 100$). We obtained $P_g$ and $T_m$ from field-test data. A normalized temperature coefficient of -0.4%/°C and a $\eta$ of 17.4% (world-record module efficiency for Si solar cells) at 25°C were used for $\eta_s$ in eqs. (10) and (11).

The output energy of a concentrator PV system is expressed by

$$P_{out} = K_T \cdot K_f \cdot P_d \cdot \eta_s , \qquad (12)$$

where $P_d$ is the direct irradiation. When the standard temperature is set to 25°C, the correction coefficient for temperature $K_T$ is

$$K_T = 1 + a\,(T_{m(con.)} - 25), \qquad (13)$$

where $T_{m(con.)}$ [$^{o}$C] is the module temperature for the concentrator system. We obtained $P_d$ from field-test data. For concentrator PV systems, $K_f$ is mainly determined by optical loss. $K_f$ for the 400 sun concentrator system using a Fresnel lens is 0.927 [19]. Therefore, we used this value as $K_f$. The temperature of the concentrator module ($T_{m(con.)}$) is experimentally given by [20]

$$T_{m(con.)} = T_m + 17\,P_d\,. \qquad (14)$$

A temperature coefficient of -0.141%/ $^{o}$C and a $\eta_s$ of 34.4% measured experimentally (obtained in this study) were used for the estimation of the 17 sun concentrator system. A temperature coefficient of -0.098%/ $^{o}$C and a $\eta_s$ of 36.7% measured experimentally (obtained in this study) were used for the estimation of the 200 sun concentrator system. The temperature coefficient and $\eta_s$ described in this study are the data for 100 mW/cm$^2$ direct irradiation. In an actual environment, the direct irradiation is almost always less than 100 mW/cm$^2$. It is considered that, in most cases, the triple-junction cells of 17 sun and 200 sun concentrator systems operate at less than 17 sun and 200 sun concentration ratios. Therefore, the temperature coefficient and $\eta_s$ were corrected depending on direct irradiation by interpolating the data in Table 1 and 2.

Using these methods, the annual output of the flat-plate and concentrator PV systems were estimated as shown in Fig. 4. The estimated annual output of the concentrator systems is higher than that of the nonconcentration system. The annual output of the 200 sun concentrator system is higher than that of the 17 sun concentrator system. Although the system becomes increasingly more complex, concentrator systems with a higher concentration ratio will attain excellent performance because of its increasing cell efficiency and superior temperature coefficient. Moreover, a higher output energy can be expected in high direct-irradiation areas such as Miami (USA) or the Great Sandy Desert (Australia) [21].

## 5. CONCLUSIONS

The temperature dependences of the electrical characteristics of InGaP/InGaAs/Ge triple-junction solar cells under concentration were evaluated. The temperature dependence of $\eta$ is mostly affected by the temperature dependence of $V_{oc}$. $\eta$ decreased with increasing temperature, and increased with increasing concentration ratio because of the increase in $V_{oc}$. The normalized temperature coefficients of the conversion efficiency ($(d\eta/dT)/\eta_{(25°C)} \times 100$) of the InGaP/InGaAs/Ge triple-junction solar cell is -0.248%/$^{o}$C at 1 sun and -0.098%/$^{o}$C at 200 suns. The decrease in $\eta$ with increasing temperature decreases with increasing concentration ratio. These results indicate that concentration operations have beneficial effects on high-temperature operations.

Moreover, the annual output of a concentrator system with a high-efficiency triple-junction cell is estimated using the experimental characteristics of solar cell obtained in this study and field-test meteorological data collected for one year at NAIST, and compared with that of a nonconcentration flat-plate system. We found that the annual output of concentrator systems composed of high-efficiency InGaP/InGaAs/Ge triple-junction solar cells was higher than that of flat-plate systems composed of Si solar cells, because of the high efficiency and superior temperature coefficient of the former systems.

## ACKNOWLEDGMENTS

This work was partially supported by the New Energy and Industrial Technology Development Organization under the Ministry of Economy, Trade and Industry, Japan.

## REFERENCES


1) J. M. Olson, S. R. Kurtz and A. E. Kibbler: Appl. Phys. Lett. 56 (1990) 623.

2) T. Takamoto, T. Agui, E. Ikeda and H. Kurita: Proc. the 28th IEEE Photovoltaic Specialists Conf., Anchorage, (2000) 976.

3) H. L. Cotal, D. R. Lillington, J. H. Ermer, R. R. King and N. H. Karam: Proc. 28th IEEE Photovoltaic Specialists Conf., Anchorage, (2000) 955.

4) A. W. Bett, F. Dimroth, G. Lange, M. Meusel, R. Beckert, M. Hein, S. V. Riesen and U. Schubert: Proc. 28th IEEE Photovoltaic Specialists Conf., Anchorage, (2000) 961.

5) C. J. Gelderloos, C. Assad, P. T. Balcewicz, A. V. Mason, J. S. Powe, T. J. Priest and J. A. Schwartz: Proc. 28th IEEE Photovoltaic Specialists Conf., Anchorage, (2000) 972.

6) M. J O'Neill, A. J. McDanal, M. F. Piszczor, M. I. Eskenazi, P. A. Jones, C. Carrington, D. L. Edwards and H. W. Brandhorst: Proc. 28th IEEE Photovoltaic Specialists Conf., Anchorage, (2000) 1135.

7) D. D. Krut, G. S. Glenn, B. Bailor, M. Takahashi, R. A. Sherif, D. R. Lillington and N. H. Karam: Proc. 28th IEEE Photovoltaic Specialists Conf., Anchorage, (2000) 1165.

8) K. Araki, H. Uozumi and M. Yamaguchi, Proc. the 29$^{th}$ IEEE Photovoltaic Specialists Conf., New Orleans, (2002) 1568.

9) S. M. Sze, "Physics of Semiconductor Devices", (Wiley-Interscience Publication), (1981) 833.

10) A. L. Fahrenbruch and R. H. Bube, "Fundamentals of Solar Cells", (Academic Press, Inc.), (1983) 238-239

11) M. J. O`Neill et al., Proc. 28th IEEE Photovoltaic Specialists Conf., Anchorage, (2000) 1161.

12) V. D. Rumyantsev et al., Proc. 28th IEEE Photovoltaic Specialists Conf., Anchorage,

(2000) 1169.

13) S. M. Sze, Physics of Semiconductor Devices 2nd ed., (Wiley-Interscience Publication), (1981) 831-833.

14) A. L. Fahrenbruch and R. H. Bube, Fundamentals of Solar Cells, (Academic Press, Inc.), (1983) 238.

15) Sarah R. Kurtz, P. Faine and J. M. Olson, J. Appl. Phys, **68** (1990) 1890.

16) D. J. Friedman, Proc. 25th IEEE Photovoltaic Specialists Conf., Washington, D.C., (1996) 89.

17) S. Yoon, and V. Garboushian, Proc. First World Conference on Photovoltaic Energy Conversion, (1994) 1500-1504.

18) K. Nishioka, T. Hatayama, Y. Uraoka, T. Fuyuki, R. Hagihara, M. Watanabe, Solar Energy Materials and Solar Cells, **75/3-4** (2002) 665-671.

19) M. Kondo, K. Araki, H. Uozumi, S. Kenmoku and M. Yamaguchi, Proc. 11th PV workshop - Japan, (2003) 49.

20) K. Araki, H. Uozumi and M. Yamaguchi, Proc. the 29th IEEE Photovoltaic Specialists Conf., New Orleans, (2002) 1568.

21) T. Kosugi, P. S. Pak, Y. Suzuki, The Transactions of The Institute of Electrical Engineers of Japan, Vol.118-B, No.3, Mar. (1998) 246.

Fig. 1. Schematic illustration of InGaP/InGaAs/Ge triple-junction solar cell.

Fig. 2. Temperature dependence of characteristics ((a) $V_{oc}$, (b) $I_{sc}$, (c) *FF* and (d) conversion efficiency) of InGaP/InGaAs/Ge triple-junction solar cell.

Fig. 3. Diffuse irradiation and direct irradiation for each month monitored at NAIST.

Fig. 4. Estimated annual output energies of concentrator PV system with triple-junction cell and flat-plate PV system with Si cell.

Table 1 Cell characteristics at 25°C for various concentration ratios.

| | $V_{oc}$ (V) | $J_{sc}$ (mA) | *FF* | η (%) |
|---|---|---|---|---|
| **1sun** | 2.53 | 6.74 | 0.849 | 29.5 |
| **17 suns** | 2.82 | 113 | 0.890 | 34.4 |
| **200 suns** | 3.05 | 1362 | 0.883 | 37.0 |

Table 2 Temperature coefficients of InGaP/InGaAs/Ge triple-junction cell's characteristics ($dX/dT$: $X$ means $V_{oc}$, $I_{sc}$, $FF$ and $\eta$) and temperature coefficients normalized by the same parameter at 25°C ($(dX/dT)/X_{(25°C)} \times 100$).

| | **1 sun** | **17 suns** | **200 suns** |
|---|---|---|---|
| $\frac{dV_{oc}}{dT}$ [V/°C] | -0.0062 | -0.0054 | -0.0046 |
| $\frac{1}{V_{oc(25^oC)}}\frac{dV_{oc}}{dT}\times 100$ [%/°C] | -0.245 | -0.191 | -0.151 |
| $\frac{dI_{sc}}{dT}$ [mA/°C] | 0.005 | 0.139 | 1.637 |
| $\frac{1}{I_{sc(25^oC)}}\frac{dI_{sc}}{dT}\times 100$ [%/°C] | 7.42 x $10^{-2}$ | 12.28 x $10^{-2}$ | 12.02 x $10^{-2}$ |
| $\frac{dFF}{dT}$ [/°C] | -0.0006 | -0.0005 | -0.0004 |
| $\frac{1}{FF_{(25^oC)}}\frac{dFF}{dT}\times 100$ [%/°C] | -7.07 x $10^{-2}$ | -5.62 x $10^{-2}$ | -4.53 x $10^{-2}$ |
| $\frac{d\eta}{dT}$ [%/°C] | -0.073 | -0.0486 | -0.0363 |
| $\frac{1}{\eta_{(25^oC)}}\frac{d\eta}{dT}\times 100$ [%/°C] | -0.248 | -0.141 | -0.098 |

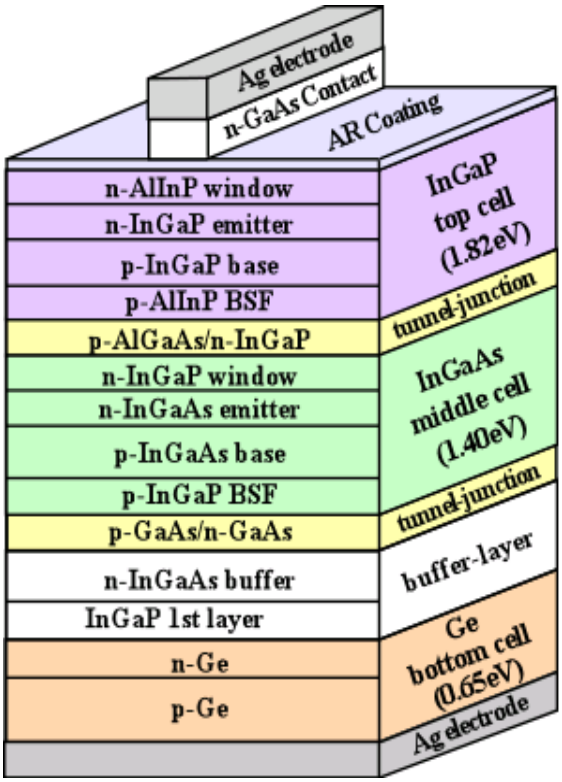


Fig. 1

K. Nishioka

**(a)**

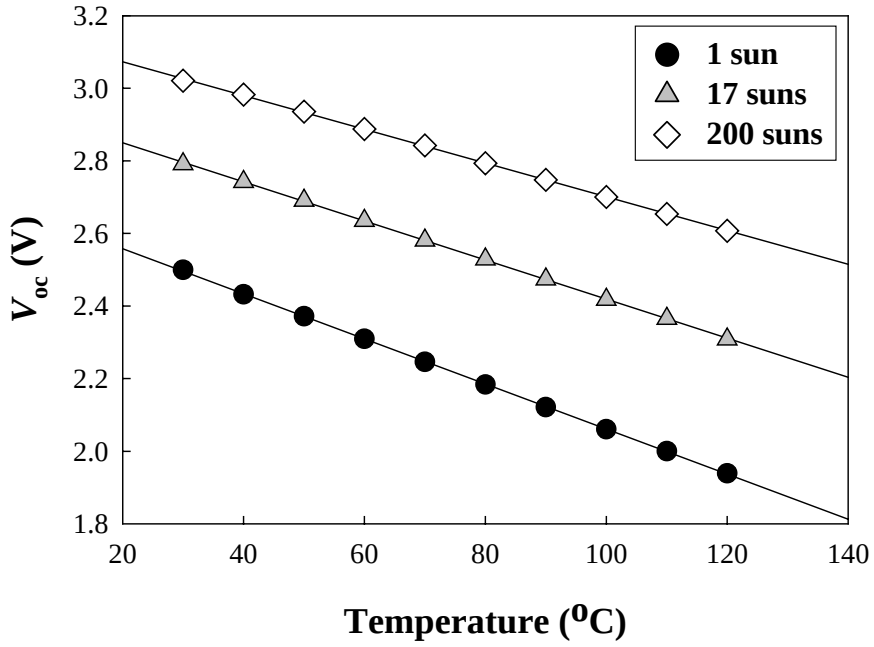


**(b)**

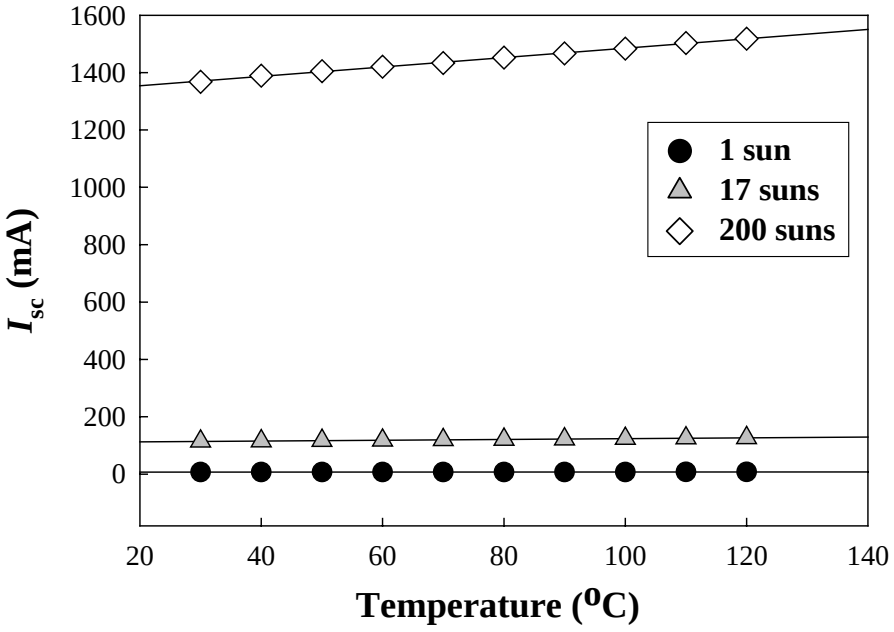


Fig. 2.

K. Nishioka

**(c)**

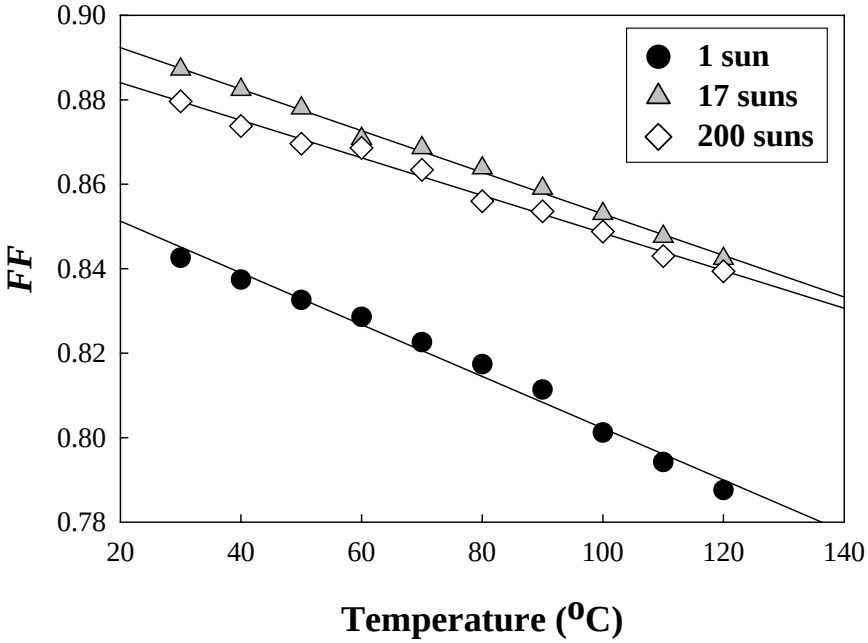


**(d)**

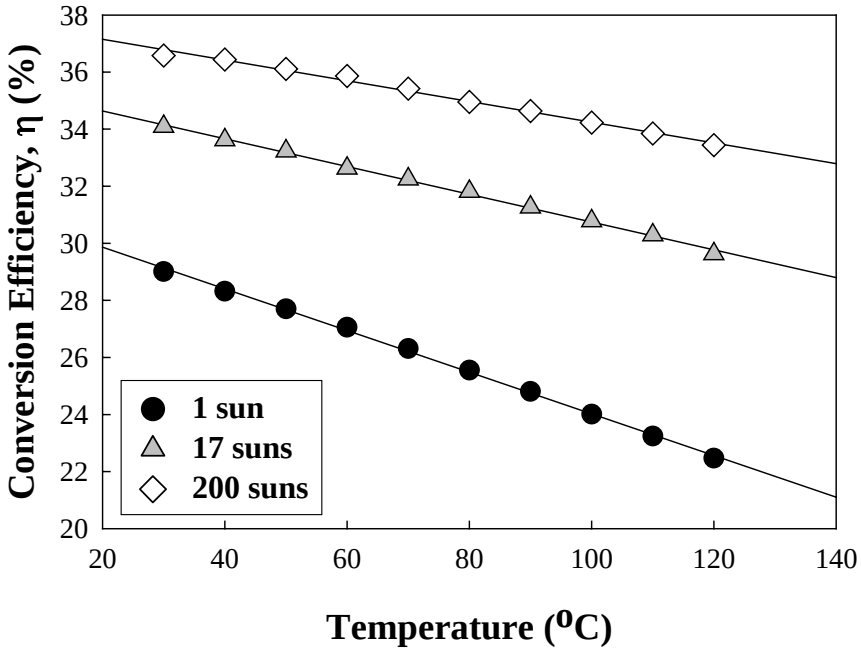


Fig. 2. K. Nishioka

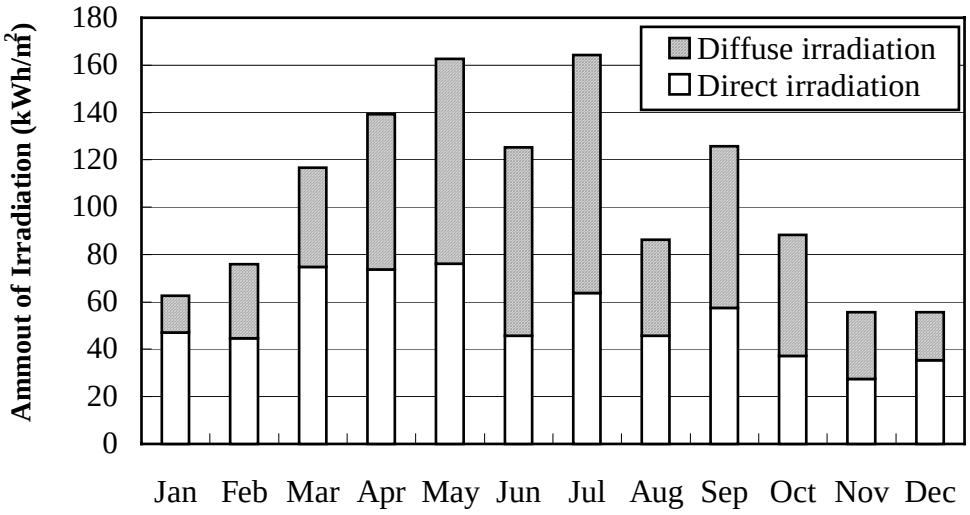


Fig. 3

K. Nishioka

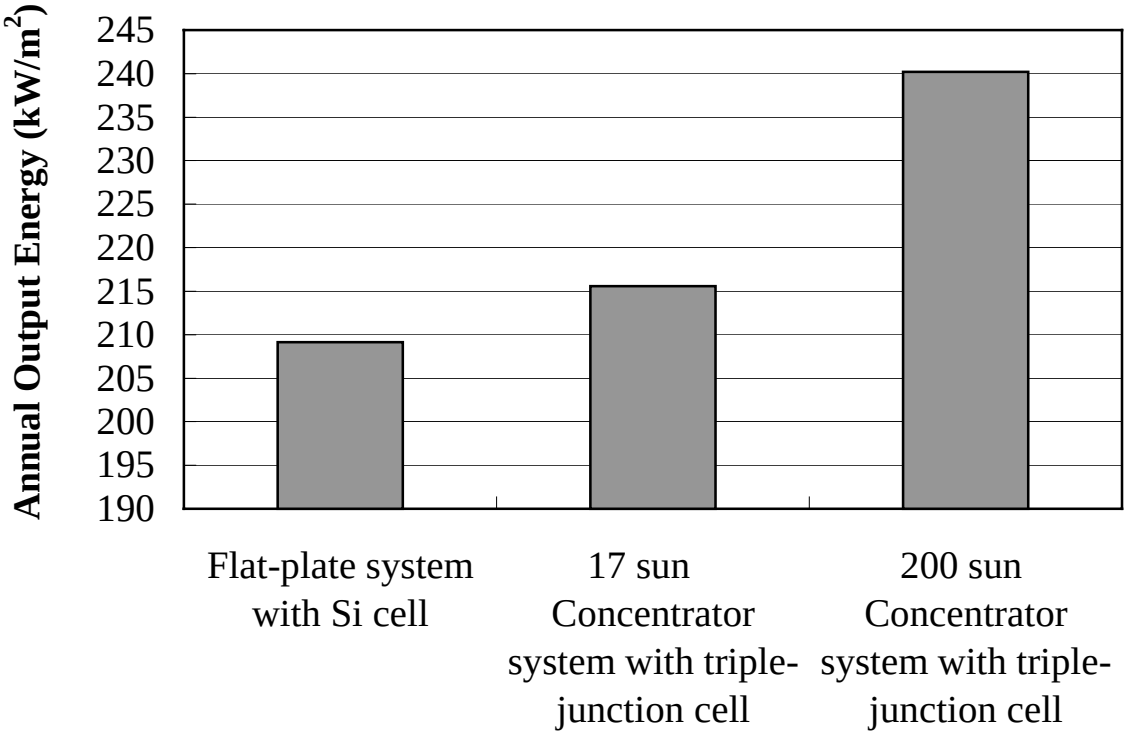


Fig. 4

K. Nishioka